



# The mystery of striated cloud heads in satellite imagery

R. S. Dixon<sup>1</sup>, K. A. Browning<sup>1</sup> and G. J. Shutts<sup>2</sup>

<sup>1</sup>*Joint Centre for Mesoscale Meteorology, Department of Meteorology, University of Reading*

<sup>2</sup>*Meteorological Office, Bracknell*

**Summary:** Striated cloud heads are associated with some of the most extreme cases of rapid cyclogenesis. Animations of two clear examples are presented and one is interpreted in detail in the light of a Limited Area Model analysis. Six alternative dynamical explanations are considered but none satisfactorily fits all the evidence.

**Keywords:** Satellite imagery, cyclogenesis, cloud heads, cloud striations

## 1. INTRODUCTION

Figure 1 shows an example of a cloud head over the mid-Atlantic as seen in infra-red imagery from the satellite Meteosat. The cloud head is the overall cloud system occupying much of the left-hand (western) half of the figure. The larger cloud system with colder (higher) cloud tops, occupying the right-hand (eastern) half of the figure is the polar front cloud band. The term cloud head was first used by Böttger *et al.* (1975) who recognized it as it as a feature that frequently precedes a period of rapid cyclonic development. The relationship of cloud heads to the overall structure and dynamics of the associated cyclone is described in Browning and Roberts (1994) and Bader *et al.* (1995). Cloud heads have been shown to be prominent features of several notable cyclones, a memorable one in north-west Europe being the Great Storm of October 1987 (Shutts, 1990). The identification of cloud heads in satellite imagery now plays an important role in operational forecasting practice (e.g. Young and Grahame 1999).

The particular feature of the cloud head in Figure 1 that will be stressed in the present study is the series of striations in cloud-top height (temperature). Striations in cloud heads were first mentioned by Shutts (1990) and Norris and Young (1991); the striations described by Shutts had a characteristic wavelength of 10 km, whereas the wavelength of those described by Norris and Young, like those in the present study, are much longer. Five of the striations are labelled A, B, C, D and E and four can be tracked throughout the 2-hour sequence of images in Figure 1. They extend radially outward

across the width of the cloud head, roughly at right angles to the outer boundaries of both the cloud head and the band of higher polar-front cloud to the east.

The striations on this, as on other occasions, are not just fleeting features in the cloud head structure; indeed some individual striations could be followed for over 5 hours. By viewing the imagery in a frame of reference moving with the cloud head, the individual striations can be seen forming at the upwind (south-western) end of the cloud head, then moving through the cloud head and decaying at its downwind (north-eastern) end. Individual striations travel at a velocity of about 50 m/s relative to the ground. They have a wavelength of about 60 km and their maximum length and crest-to-trough amplitude are 250 km and approximately 1.4 km, respectively. Similar striations have been observed in many lows by Feren (1995) who regarded them as an indication of strong winds and rapid deepening; of the 37 lows that exhibited what Feren called a “striated delta” cloud structure, 75% were associated with at least gale-force winds and most exhibited a 12-hour period of explosive deepening. Gales and explosive deepening also characterized the case shown in Figure 1: this is the storm that crossed the United Kingdom on 24 December 1997, accompanied by surface winds gusting in some places to in excess of 40 m/s. The cyclone with which the cloud head was associated deepened by 23 mb in 12 hours during its period of most rapid development.

In the next section we present a more detailed analysis of another example of cloud-head striations and then in section 3 we discuss possible mechanisms for their generation.

## 2. CASE STUDY OF CLOUD-HEAD STRIATIONS ON 25 DECEMBER 1998

The event shown in Figure 2 occurred over the north Atlantic during Christmas Day in 1998. A feature of this case is that six partially overlapping cloud heads exist simultaneously. These are marked 1 to 6 in Figure 3. Some of the cloud heads again show striations in the cloud tops although the striations are only about half the length of those in the previous example in Figure 1. As in the previous example, the striations can be tracked as they progress through the cloud head. Figure 2 shows an animation between 1200UTC and 1530UTC, with imagery every 30 minutes. We concentrate our attention on the striations within Cloud Head 5. Five striations (A to E) have been analysed, the ends of which are annotated within Figures 2 and 3 (note that the labels are at the south-eastern ends of the striations rather than the north-western ends as was the case in Figure 1). At 1300UTC, the sun’s angle was such that visible imagery from Meteosat (not shown) was able to reveal the surface cold front associated with Cloud Head 5 as a line of bright cloud tops that characterize line convection at the surface (as in figure 1 of Browning and Harrold, 1970).

Several properties of the striations can be defined, as shown in the schematic in Figure 4. Table 1 shows characteristic values for these variables. The speed of travel of the striations varies from striation to striation and with time. The striations travel most slowly in their early stages of

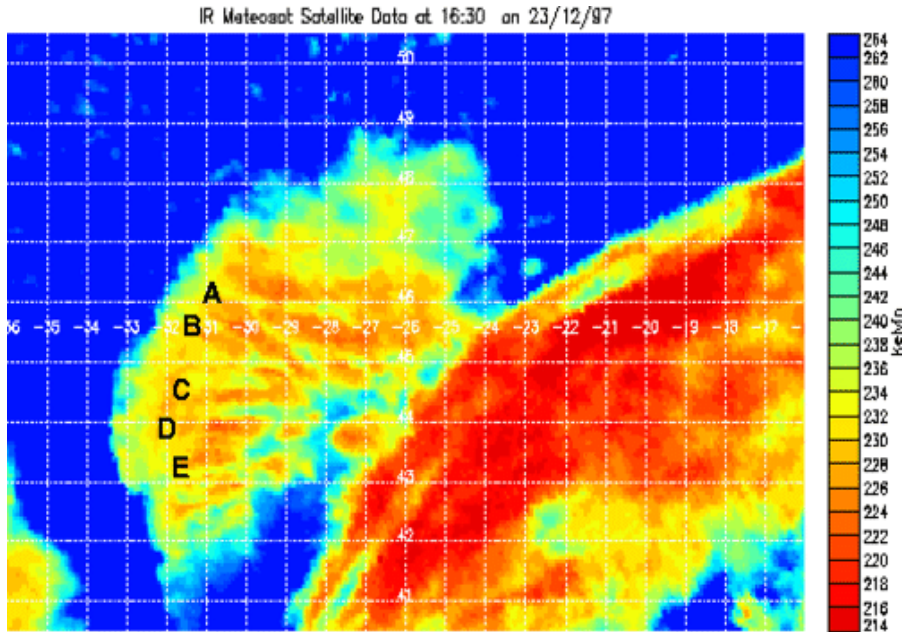


**Figure 1.** Animation of false colour infra-red Meteosat imagery in half-hourly intervals between 1630UTC and 1900UTC on 23 December 1997. A, B, C, D and E show the positions of striations as they move through the cloud head.

development. Average speed varies from approximately 48 m/s for Striation A to 41 m/s for Striation E. As in the case described in the introduction, the striations form at the upwind (south-western) end of the cloud heads and then move through the cloud heads to decay at their downwind end. The tops of the crests of the striations tend to become rather flattened with time. The flat top of Striation C is about 15 km wide at 1200UTC and is 50 km wide by 1530UTC. The average horizontal wavelength of the striations increases with time from 30 to 55 km. The wavelength also increases from Striation E through to Striation A at any given time.

Figure 5a shows the pattern of cloud-top temperature as determined from the 12UTC operational analysis of the U.K. Met. Office Limited Area Model (LAM). Figure 5b shows the model-derived thermodynamic structure in the vicinity of the striations. The “X” in Figure 5a shows the position of this temperature profile in relation to the model’s own representation of the field of cloud-top

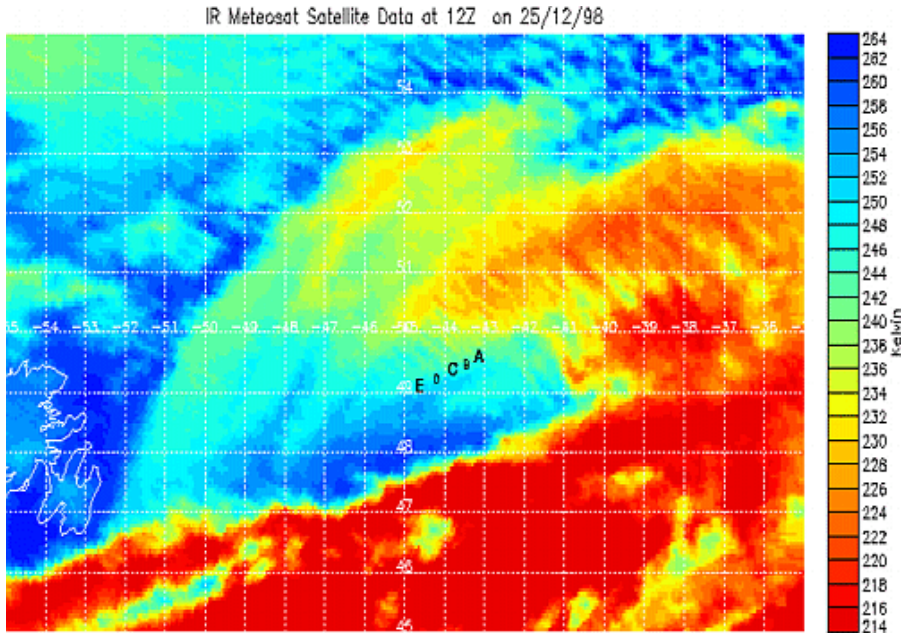


**Figure 2.** As Figure 1 but for half-hourly infra-red Meteosat imagery from 1200UTC to 1530UTC on 25 December 1998. A, B, C, D, E label striations as they advance through the cloud head but B and D are labelled only at the initial time. This lettering is referred to in later figures.

temperature. Comparison of Figure 5a with Figure 2 shows that the model, whilst not resolving the individual striations or indeed details of the multiple cloud-head structure, successfully represents the overall structure of the cloud-head region, albeit with a positional error (the model's cloud head is about 150 km too far north-northeast but this has been taken into account in finding the position X in the model that is relevant to the observed striations).

According to Figure 5b, the cloud head is associated with an exceptionally strong and deep frontal zone extending between 800 and 500 mb. Across this layer the potential temperature increases by as much as 23 K, whilst the south-westerly winds increase from 5 to 65 knots (about 2 to 32 m/s). The shear in the model is orientated almost parallel to the elongated cloud head and its associated frontal zone. The wind continues to increase above 500 mb, reaching 100 knots (50 m/s) in the dry air at

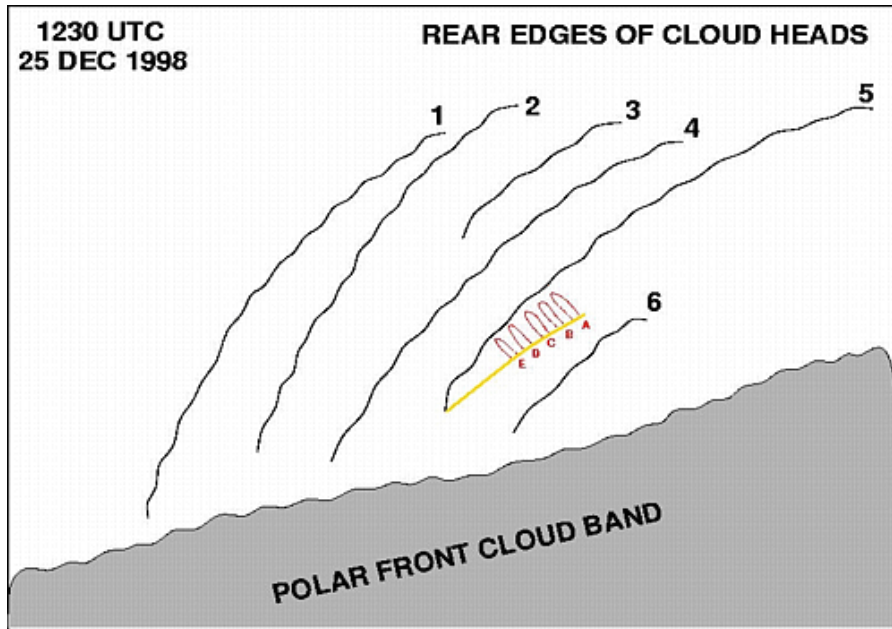


**Figure 3.** Sketch of 1230 UTC image from [Figure 2](#) showing the polar front cloud band (shaded) and the rear edges of the six partially overlapping cloud heads. The cloud striations A, B, C, D and E analysed in this study were associated with Cloud Head 5 and are drawn red. The yellow line connecting the south-eastern ends of these striations, extending to the south-western tip of Cloud Head 5, denotes the band of line convection that was observed along the south-eastern edge of Cloud Head 5.

350 mb. Between this dry air and the essentially saturated air in the frontal zone, there is a layer of almost constant wet-bulb potential temperature ( $\theta_w$ ), with a slight decrease in relative humidity, from 500 to 420 mb. The temperature profile in [Figure 5b](#) is representative of the developing striations towards the upwind end of the train of striations (i.e. Striation D at 1230UTC ([Fig. 3](#))). In this region, the observed temperatures at the crests and troughs are typically 233 K and 243 K ([Fig. 2](#)). This is consistent with the cloud-top striations being situated within the constant- $\theta_w$  layer between 500 and 420 mb, as labelled in [Figure 5b](#), and gives a typical cloud-top height,  $h$ , of approximately 6 km and a crest-trough amplitude of approximately 1.4 km.

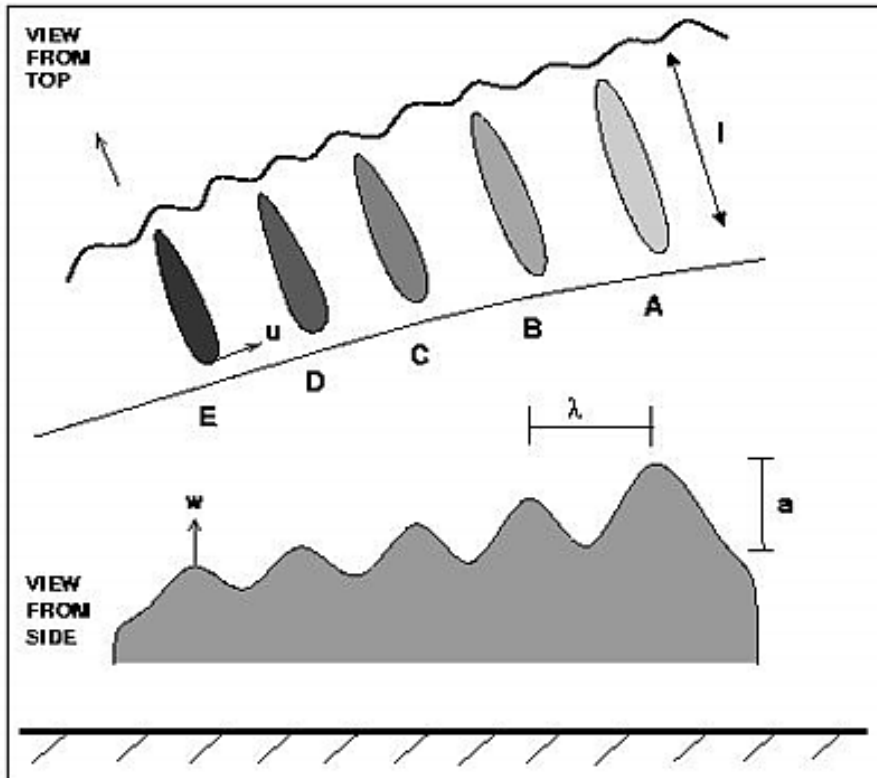


**Figure 4.** Schematic representation of the cloud striations A, B, C, D and E associated with Cloud Head 5 as viewed from the top and the side. The striations A, C and E have been analysed to determine their length  $l$ , cloud-top height  $h$ , along-cloud-head velocity  $u$ , cloud-top rate of ascent  $w$ , characteristic horizontal wavelength  $\lambda$  and crest-to-trough amplitude  $a$ .

Figure 2 suggests some degree of coherence in the striations within adjacent cloud heads. Since the flows associated with the adjacent cloud heads are partially overlapping, this would not be surprising. However, the wavelengths of the striations in neighbouring cloud heads are not identical, so there is inevitably also a degree of mismatch between their striations.

**Table 1.** Summary of characteristics of striations within Cloud Head 5 in figure 2 (see figure 4 for definitions)

Variable	Summary of characteristics
Wavelength $\lambda$	30 km (at 1200 UTC) to 55 km (at 1500 UTC) averaged over all the striations
Crest-to-trough amplitude $a$	Typically 1 km, maximum of approx. 2 km (e.g C at 1400 UTC)
Length $l$	Between 70 km (e.g. E at 1200 UTC) and 140 km (C at 1530 UTC)
Ground-relative velocity $u$	A: 41 m/s (1200 UTC) to 52 m/s (1400 UTC), average=48 m/s C: 39 m/s (1200 UTC) to 55 m/s (1430 UTC), average=46 m/s E: 33 m/s (1200 UTC) to 47 m/s (1500 UTC), average=41 m/s
Cloud-top height $h$	A: 6.5 km at 1200 UTC to 9 km at 1430 UTC C: 6.2 km at 1200 UTC to 9 km at 1530 UTC E: 5.5 km at 1200 UTC to 7.7 km at 1530 UTC
Vertical velocity $w$	Approx. 16 cm/s averaged over 3.5 hours for A,C,E

### 3. DISCUSSION

Here we consider candidate mechanisms that may have been responsible for the striations within the cloud heads.

#### 3.1 Conditional symmetric instability (CSI)

Bennetts and Hoskins (1979) showed that mesoscale bands of ascent within frontal systems may be due to the release of CSI. This manifests itself as rolls along the thermal wind. The LAM data suggest that the thermal gradients in this example are aligned WSW–ENE and thus any bands due to CSI should be oriented in this direction. The striations in this case are, however, orientated NNW–SSE and cannot be attributed to CSI. On the other hand, it is possible that the multiplicity of observed cloud heads, which is symptomatic of a multiplicity of transverse circulations, may be due to CSI: certainly values of Slantwise Convective Available Potential Energy (SCAPE) as high as 2500 J/kg were diagnosed from the numerical weather prediction (NWP) model on this occasion (Dixon *et al.*, 2000). The failure of the model fully to resolve the multiple cloud heads can be attributed to the coarseness of its (50 km) grid (Persson and Warner, 1993).

#### 3.2 Line convection

As mentioned in section 2, the visible imagery indicated the existence of line convection at the south-eastern ends of the striations. Although the resolution of the imagery is insufficient to resolve

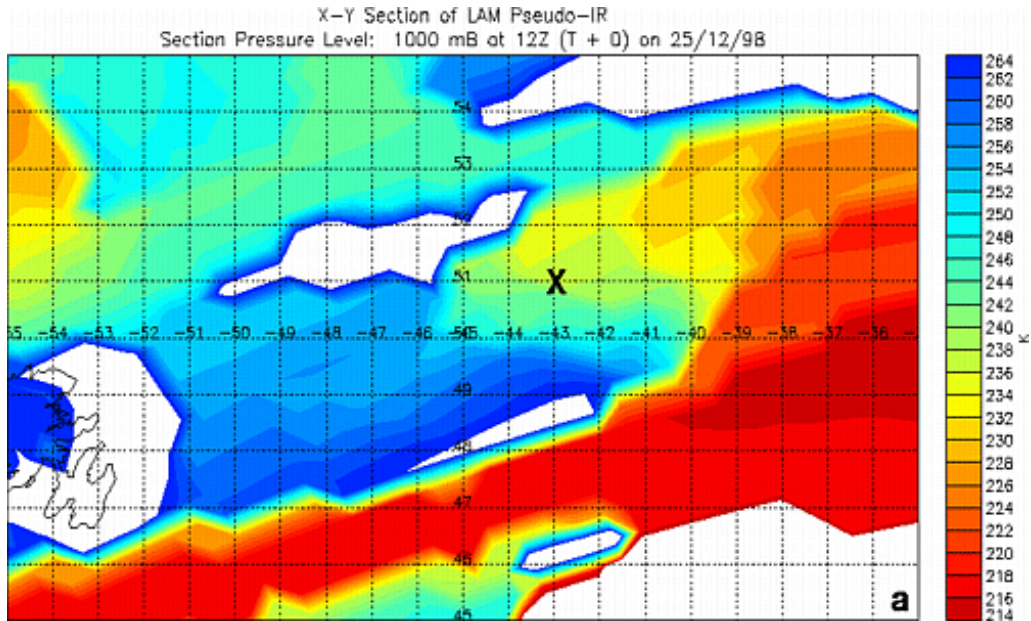


**Figure 5 (a).** Pseudo infra-red image for the area corresponding to Figure 2 from the LAM analysis at 1200UTC. Cross shows the position of the tephigram in (b overleaf). Each half, full and solid wind barb in (b overleaf) corresponds to a windspeed of 5, 10 and 50 knots, respectively.

the fine structure of the line convection, James and Browning (1979) and Hobbs and Biswas (1979) have shown that the surface cold-frontal ascent at line convection tends to be split up into cores of stronger ascent along the length of the front. These cores, or line elements, vary in length, but a length of several tens of kilometres would not be unusual. Satellite imagery in Dixon (2000) showed how these convective cores might feed plumes of slantwise ascent. As they rise behind the front, these plumes are drawn out in the along-front direction by the background geostrophic vertical shear. As suggested by satellite observations in the study by Dixon, this causes the plumes to be orientated at angles approximately 30 degrees to the thermal wind. The striations in the present study are at 90 degrees to the thermal wind, which suggests that they are not due to plumes emanating from the line convection.

Data: Column from LAM  
12Z (T + 0) on 25/12/98  
Lat: 51.00 Lon: -43.00

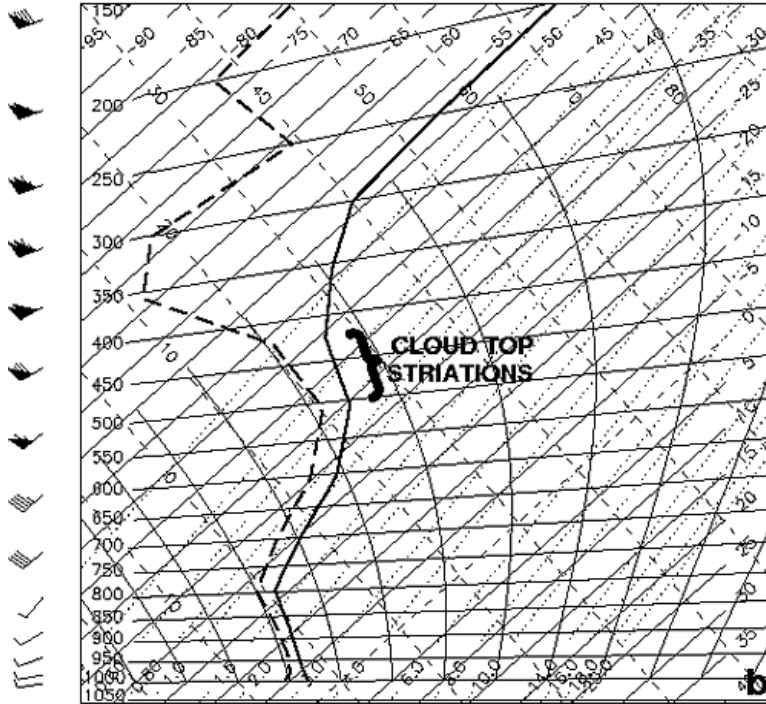


Figure 5 (b).

### 3.3 Convective rolls

The organization of boundary-layer convection into long roll clouds aligned approximately in the direction of the mean wind shear is commonly observed in satellite imagery (e.g. in the polar air as it flows off an ice sheet over relatively warm seas). If the air ascending slantwise is conditionally unstable, as it might be in the layer between 500 mb and 420 mb in Figure 5a, and this instability is

released during uplift, then similar convective rolls could result at these upper levels. As time goes on, the tops of the convective rolls would reach the base of the overlying stable layer and could be expected to flatten, as observed in this case.

This interpretation of the cloud striations would hold only if the wind shear were dominated by the ageostrophic, slantwise-ascending flow. However, in this case, at least in the model, the shear is dominated by the thermal wind shear which is normal to the orientation of the striations. It may be, however, that the smallness of the wind-component in the cross-frontal plane, shown by the wind barbs in [Figure 5b](#), is because the model is not able to resolve the augmentation of the frontal circulation by symmetric instability.

The separation of convective cloud rolls is proportional to the depth of the unstable layer and for boundary-layer rolls would be typically about 10 km (e.g. [Wallace and Hobbs, 1977](#)). Whilst this separation is not inconsistent with the separation of the striations found in the October 1987 storm ([Shutts, 1990](#)), it is too small to account in a straightforward way for the observations here. On the other hand, it appears that the depth of a convecting layer is not the only factor in determining the spacing of cloud updraughts. Mesoscale cellular convection over the ocean frequently has cell diameters of 40 km in a convecting layer 1–2 km deep. There is evidence from numerical modelling studies (e.g. [Fiedler, 1990](#)) that convection cells can grow in horizontal extent by cell merging, particularly for three-dimensional cell organization. It may be that the increase in striation separation as time progresses is a manifestation of a similar scale-broadening process.

### 3.4 Kelvin–Helmholtz Instability (KHI)

Another possibility is that the striations may be related to KH billows occurring within the strongly sheared frontal zone. In the model, the main component of the shear appears to be due to the thermal wind. The attraction of invoking KHI is that the orientation of the observed striations is consistent with the expected orientation of any billows in this zone (although this assumes that the flow pattern in the model is broadly correct, which, as noted above, may not be the case). A necessary condition for KHI is that the Richardson number ( $R_i$ ) is less than 0.25 ([Miles and Howard, 1964](#)). For a sheared layer of finite thickness  $\Delta z$ , the fastest growing wavelength for billows is given by [Miles and Howard \(1964\)](#) as  $\lambda = 7.5z$ . Inspection of the vertical profile in [Figure 5a](#) shows that there is, at most, a 4-km-deep frontal zone. If the instability were to exist over the whole of this depth (most unlikely) then the instability would be manifest with a wavelength of 30 km, which is too small compared to the wavelengths shown in [Table 1](#). Indeed, inspection of the moist Richardson number in the U.K. Meteorological Office's Limited Area Model suggests that values of  $R_i$  fall below 1 only over a layer about 1 km thick. Thus KHI does not account for the observed striations.

### 3.5 Spike clouds

Scorer (1997) has identified a banded cloud structure that commonly occurs in the upper part of frontal zones and refers to these as “spike clouds”. They frequently appear as sharp inverted-V patterns pointing up the frontal surface—often with their pointed ends close to the periphery of a cirrus cloud shield. The separation between individual spikes is typically 30–40 km, i.e. similar to that of the striations shown in this paper. It is difficult to say whether or not the underlying dynamical mechanism for these clouds may be the same as for the present striations, though it should be noted that they both grow in environments of weak slantwise stability. Scorer himself only goes as far as relating the generation mechanism to the inherent instability of three-dimensional vortex tubes.

The tendency of cirrus fallstreaks to lie normal to the thermal wind shear was discussed by Ludlam (1980). From careful visual observations he concluded that these cirrus-fallstreak cloud systems lay within layers of intense ageostrophic shear resulting from the adjustment of jet streaks. The ageostrophic shear would therefore appear to be the main contributor to the total shear in Ludlam’s study and falling ice crystals would trail along the total shear vector at right angles to the flow. In the present study, however, the wind shear is dominated by the thermal wind component unless, as described above, the model is underestimating the transverse circulation due to its inability to resolve the release of CSI.

### 3.6 Gravity waves

The spatially periodic form of the striations in our study is reminiscent of trapped lee waves, though with horizontal wavelengths somewhat larger than ones generated by mountains. The horizontal energy propagation necessary to allow such a wavetrain would be possible only if wave energy were effectively trapped near the frontal surface. How this might be achieved when the striations appear to be travelling with a speed not greatly different from that of the flow at their level is hard to see and represents the principal objection to this dynamical mechanism. It is also difficult to understand why trapped gravity waves would become aligned transverse to the front when the most obvious forcing mechanism is the line convection itself. Feren (1995) suggests the possibility that the waves are associated with geostrophic adjustment near upper jet streaks, i.e. the Lighthill radiation mechanism discussed in a shallow-water equation context by Ford (1994). The striations observed by Shutts (1990) were seen to emanate from line convection in the lower troposphere, becoming indistinct in the upper troposphere, and therefore making this process an unlikely dynamical candidate. Nevertheless the possibility that a quasi-balanced frontal surface being drawn into a vortex could excite gravity waves is interesting.

## 4. CONCLUSIONS

The discussions of possible mechanisms in this study are based on an NWP analysis which, although capable of representing the existence of the cloud head with which the striations are associated, cannot be relied upon to represent critical details. The balance of evidence is arguably in favour of the striations being due to convective rolls occurring above a frontal zone in the presence of a strong ageostrophic circulation grossly under-resolved by the model. There were no in situ observations of the wind and thermal structure in this or, as far as we know, any other striated cloud head and, until there are, their cause will remain a mystery. The cases studied in this paper are some of the clearest examples of striated cloud-heads we have seen and our purpose in showing them is to stimulate the search for better observations and theories. Striated cloud heads accompany some of the most extreme cases of rapid cyclogenesis and so this is a mystery of some practical significance.

### Acknowledgements

We would like to thank David Schultz for comments on an early version of this paper. We are also grateful to Ian Watkins for the code enabling the manual animation of the satellite imagery in figures 1 and 2.

### References

- Bader, M. J., Forbes, G. S., Grant, J. R., Lilley, R. B. E. and Waters, A. J., 1995. *Images in weather forecasting*. Cambridge, U.K.: Cambridge University Press, 499pp.
- Bennetts, D. A. and Hoskins, B. J., 1979. Conditional symmetric instability—a possible explanation for frontal rainbands. *Q. J. R. Meteorol. Soc.*, **105**, 945–962.
- Böttger, H., Eckhardt, M. and Katergiannakis, U., 1975. Forecasting extratropical storms with hurricane intensity using satellite information. *J. Appl. Meteor.*, **14**, 1259–1265.
- Browning, K. A. and Harrold, T. W., 1970. Air motion and precipitation growth at a cold front. *Q. J. R. Meteorol. Soc.*, **96**, 369–389.
- Browning, K. A. and Roberts, N. M., 1994. Structure of a frontal cyclone. *Q. J. R. Meteorol. Soc.*, **120**, 1535–1557.
- Dixon, R. S., 2000. *Diagnostic studies of symmetric instability*. Ph.D Thesis.
- Dixon, R. S., Browning, K. A. and Shutts, G. J., 2000. Aspects of the observed evolution of cloud heads. Submitted to *Q. J. R. Meteorol. Soc.*
- Feren, G., 1995. The striated-delta cloud system—a satellite imagery precursor to major cyclogenesis in the Eastern Australian-Western Tasman Sea region. *Wea. Forecasting*, **10**, 286–309.
- Fiedler, B. H., 1990. Transitions to broad cells in a nonlinear thermal convection system. *Geophys. and Astrophys. Fluid.*, **50**, 195–201.
- Ford, R., 1994. Gravity wave radiation from vortex trains in rotating shallow water. *J. Fluid. Mech.*, **281**, 81–118.

- Hobbs, P. V. and Biswas, K. R., 1979. The cellular structure of narrow cold-frontal rainbands. *Q. J. R. Meteorol. Soc.*, **105**, 723–727.
- James, P. K. and Browning, K. A., 1979. Mesoscale structure of line convection at surface cold fronts. *Quart. J. Roy. Meteor. Soc.*, **105**, 371–382.
- Ludlam, F. H., 1980. *Clouds and Storms*. University Park and London: The Pennsylvania State University Press.
- Miles, J. W. and Howard, L. N., 1964. Note on a heterogeneous shear flow. *J. Fluid Mech.*, **20**, 331–336.
- Norris, J. and Young, M. V., 1991. Satellite photographs—2 February 1991 at 1533 UTC. *Met. Mag.*, **120**, 115–116.
- Persson, P. O. G. and Warner, T. T., 1993. Nonlinear hydrostatic conditional symmetric instability: implications for numerical weather prediction. *Mon. Wea. Rev.*, **121**, 1821–1833.
- Scorer, R. S., 1997. *Dynamics of Meteorology and Climate*. Wiley and Sons, 686pp.
- Shutts, G. J., 1990. Dynamical aspects of the October Storm 1987: a study of a successful fine mesh simulation. *Q. J. R. Meteorol. Soc.*, **116**, 1315–1347.
- Wallace, J. M. and Hobbs, P. V., 1977. *Atmospheric Science: An Introductory Survey*. New York: Academic Press.
- Young, M. V. and Grahame, N. S., 1999. Forecasting the Christmas Eve storm 1997. *Weather*, **54**, 382–391.